Md. Shuza Uddin*, Animesh Kumer Chakraborty, Stefan Spellerberg, Ingo Spahn, Md. Asad Shariff, Md. Abdur Rashid and Syed M. Qaim

Excitation functions of proton induced nuclear reactions on ^{nat}Fe up to 16 MeV, with emphasis on radiochemical determination of low cross sections

DOI 10.1515/ract-2017-2818
Received May 4, 2017; accepted May 12, 2017; published online July 4, 2017

Abstract: Excitation functions for the formation of the radionuclides ^{56}Co, ^{57}Co, $^{58m+g}$Co and ^{54}Mn via proton induced reactions on natural iron target were measured from their respective thresholds up to 16 MeV using the stacked-foil activation technique and HPGe detector γ-ray spectroscopy. In the threshold energy range, the low cross sections for ^{54}Mn were measured radiochemically. All the measured values were compared with available experimental data and with theoretical calculations reproduced in TENDL-2015 nuclear data library. New data for the formation of ^{57}Co, ^{58}Co and ^{54}Mn were obtained near their reaction thresholds. Other data obtained strengthen the database. Polynomial fittings of the data measured in this work as well as of all data sets (including the present data) were performed. The present data appear to be closer to theoretical calculations than the literature data.

***Corresponding author: Md. Shuza Uddin,** Tandem Accelerator Facilities, Institute of Nuclear Science and Technology, Atomic Energy Research Establishment, Savar, Dhaka, Bangladesh; and Institut für Neurowissenschaften und Medizin, INM-5: Nuklearchemie, Forschungszentrum Jülich, D-52425 Jülich, Germany, E-mail: md.shuzauddin@yahoo.com
Animesh Kumer Chakraborty: Tandem Accelerator Facilities, Institute of Nuclear Science and Technology, Atomic Energy Research Establishment, Savar, Dhaka, Bangladesh; and Department of Physics, Chittagong University of Engineering and Technology, Chittagong, Bangladesh
Stefan Spellerberg, Ingo Spahn and Syed M. Qaim: Institut für Neurowissenschaften und Medizin, INM-5: Nuklearchemie, Forschungszentrum Jülich, D-52425 Jülich, Germany
Md. Asad Shariff: Tandem Accelerator Facilities, Institute of Nuclear Science and Technology, Atomic Energy Research Establishment, Savar, Dhaka, Bangladesh
Md. Abdur Rashid: Department of Physics, Chittagong University of Engineering and Technology, Chittagong, Bangladesh

Keywords: ^{nat}Fe target, 16.7 MeV protons, stacked-foil activation technique, BC 1710 cyclotron, excitation function, radiochemical separation.

1 Introduction

Activation cross sections of charged-particle induced reactions are important both for theoretical considerations and practical applications [cf. 1–4]. In this work we measured data on iron which is used as structural material in nuclear facilities. The cross sections for the formation of long-lived radioisotopes, e. g. ^{56}Co, ^{57}Co, ^{54}Mn, etc. are needed in several areas, for example, waste disposal studies on activated accelerator components, thin layer activation analysis, preparation of calibration sources for Mössbauer spectrometry, γ-ray spectrometry and Single Photon Emission Tomography (SPECT), etc. Furthermore, several enriched isotopes of iron are used as target materials in production of non-standard positron emitters, e. g. ^{55}Co, ^{57}Ni, etc., for medical use. A few groups reported cross section data sets for several (p,x) reactions induced in the iron target, using both natural iron and a few highly enriched iron isotopes [5–23]. There are some discrepancies in the reported data and the information available near the reaction thresholds is rather weak. Two measurements using ^{nat}Fe and enriched ^{57}Fe as targets were reported previously from the Forschungszentrum Jülich [19, 22]. In the first work the emphasis was on the fundamental analysis of reaction mechanisms whereas in the second paper more accurate data for applications were presented. Recently special attention has been devoted to lower energy region (<5 MeV), and the results for ^{nat}Ni and ^{60}Ni targets have been reported [3, 24]. Now we measured the data on ^{nat}Fe with particular emphasis on the energy range near the reaction threshold. For determining very low cross sections of ^{54}Mn, radiochemical separation was performed. The data were compared with nuclear model

calculations to draw some information on the reaction mechanism.

2 Experimental

2.1 Samples and irradiations

The cross sections of the proton induced nuclear reactions on iron of natural isotopic composition were measured by the well-known stacked-foil activation technique. Each stack consisted of thin foils (10 and 25 μm) of iron target, copper monitor (25 μm) and aluminum absorber (50 μm). Several copper foils were inserted in a stack to follow the beam parameters along the stack. The 25 μm thick iron foils were placed in the front section of a stack and a number of 10 μm thin iron foils in the back part of the stack, where the energy of the proton beam was reduced to <10 MeV, to keep the energy spread in each foil to a minimum. Each foil was cut into a circular size of 13 mm diameter. Four stacks were prepared for irradiation. Three stacks were irradiated for 120 min and the fourth one for 60 min with protons of energy 16.7 MeV at the Baby Cyclotron BC1710 of the Forschungszentrum Jülich, Germany. The irradiation facility has been recently well characterized [25]. During the irradiation the beam current was 1 μA. Details related to sample preparation and irradiations have been recently described [cf. 24].

The energy of the extracted particle beam was given by the accelerator parameters. The primary energy of the protons incident on the first Cu foil was, however, determined by comparing the measured ratio of the ^{62}Zn/^{65}Zn activities [cf. 24–26] with that from the IAEA recommended excitation functions of the two relevant reactions, namely ^{nat}Cu(p,x)^{62}Zn and ^{nat}Cu(p,x)^{65}Zn [cf. 27].

The beam energy degradation along the stack was calculated using the computer program STACK which was written at the Forschungszentrum Jülich, based on the energy-range relation described by Williamson et al. [28]. The excitation functions of the monitor reactions were measured to check the beam parameters along the stack.

2.2 Measurement of radioactivity

The radioactivity of a reaction product in the activated target or the monitor foil was generally measured nondestructively using HPGe detector γ-ray spectrometry. The activity measurement was started about 4 h after the end of irradiation to allow decay of short-lived radionuclides to suppress the disturbing background in the γ-ray spectrum. To keep the dead time below 3 %, samples were counted at a distance of 20 cm, 10 cm or 3 cm from the detector surface, depending on the level of the activity. Each sample was recounted 2–3 times by giving sufficient cooling interval to check the half-life of the activation product as well as to avoid disturbance by overlapping γ-lines from undesired products. The ^{58}Co activity was measured after proper waiting time to allow complete decay of the short-lived isomeric state.

The efficiency versus energy curve of the HPGe γ-ray detector was determined using the standard point sources ^{57}Co, ^{60}Co, ^{133}Ba, ^{137}Cs and ^{152}Eu, traceable to PTB Braunschweig, Germany. The decay data of the investigated radionuclides were generally taken from the LUND/LBNL database [29]; they are given in Table 1. The threshold energy given for each reaction does not include the Coulomb barrier. The experimental reaction threshold for each activation product deduced from the respective figure is also given in Table 1.

Table 1: Decay properties of the investigated radionuclides[a] formed in the interactions of ^{nat}Fe with protons of energy < 16 MeV.

Product radionuclide	Half-life	γ-ray energy (keV)	I_γ(%)	Contributing reaction	Q-value (MeV)	Threshold energy (MeV)[b]
^{56}Co	77.27 d	846.8	100.0	^{56}Fe(p,n)^{56}Co	−5.35	5.45
		1037.8	13.9	^{57}Fe(p,2n)^{56}Co	−13.00	13.23
^{57}Co	271.79 d	122.0	85.6	^{56}Fe(p,γ)^{57}Co	6.03	0.00
		136.5	10.7	^{57}Fe(p,n)^{57}Co	−1.62	1.65
				^{58}Fe(p,2n)^{57}Co	−11.66	11.87
^{58}Co	70.86 d	810.8	99.0	^{57}Fe(p,γ)^{58}Co	6.95	0.00
				^{58}Fe(p,n)^{58}Co	−3.10	3.14
^{54}Mn	312.30 d	834.8	99.9	^{57}Fe(p,α)^{54}Mn	0.24	0.00
				^{58}Fe(p,αn)^{54}Mn	−9.83	10.00

[a]Chu et al. [29].

[b]The threshold energy given for each reaction does not include the Coulomb barrier. The experimental reaction thresholds deduced from Figures 2–5 for various activation products are: ^{56}Co(5.5 MeV); ^{57}Co(1.8 MeV); ^{58}Co(2.3 MeV); ^{54}Mn(4.8 MeV).

2.3 Radiochemical determination of ^{54}Mn

In several samples irradiated with <8 MeV protons, ^{54}Mn could not be detected due to very strong cobalt activities, especially ^{56}Co. An independent radiochemical study was therefore carried out. Two separate stacks containing the above mentioned foils (i. e. Fe, Cu and Al) were irradiated, each for 120 min with 16.7 MeV protons at 1 μA at BC 1710 in Jülich. The calculation of the effective energy for each foil as well as of the proton flux was done as described above.

After a decay period of about 6 months, radiomanganese was chemically separated using the method described by Zaman et al. [30]. Each Fe foil was dissolved in 4 mL of conc. HCl and 2 mL of H_2O_2. The solution was evaporated to dryness to remove H_2O_2, the residue was taken up in 5 mL of conc. HCl and Fe was removed by extraction with two 10 mL portions of diethyl ether saturated with conc. HCl. The aqueous solution was evaporated to dryness slowly to remove traces of ether. The residue was taken up in 10 mL of conc. HCl. It contained radiocobalt and radiomanganese at the no-carrier added level. It was then transferred to a small quartz column (ϕ = 2.0 cm, height = 10 cm) filled with the anion-exchange resin Dowex 1 × 8, chloride form, 100–200 mesh (FLUKA). The column was conditioned with 10 mL of conc. HCl, then eluted with 10 mL of 6 M HCl whereby radiomanganese was eluted. The column was finally eluted with 1 M HCl to remove the remaining activities [cf. 31].

The collected radiomanganese fraction was concentrated by evaporation to a volume of about 0.5 mL. It was transferred to a plastic vial and counted directly on the surface of a HPGe detector. The γ-ray spectrum obtained showed a clear peak of ^{54}Mn at 834.8 keV even in those samples which were obtained from ^{nat}Fe targets irradiated with <8 MeV protons (where non-destructively no ^{54}Mn was seen). A section of the γ-ray spectrum without chemical separation as well as with chemical separation of radiomanganese is reproduced in Figure 1. The spectrum showed, besides ^{54}Mn, also γ-lines of ^{56}Co and ^{58}Co. It was estimated that the radiocobalt carried in the radiomanganese fraction was <0.1 % of its total amount in irradiated ^{nat}Fe. Thus a decontamination factor of 10^3 was achieved. This meant that the background activity had considerably decreased but the chemical separation of ^{54}Mn was not very clean. Nonetheless, it was possible to determine the area under the 834.8 keV peak of ^{54}Mn accurately, i. e. without interference from the 810.8 and 846.8 keV peaks of ^{58}Co and ^{56}Co, respectively. Each separated sample was counted for at least 24 h to achieve good counting statistics.

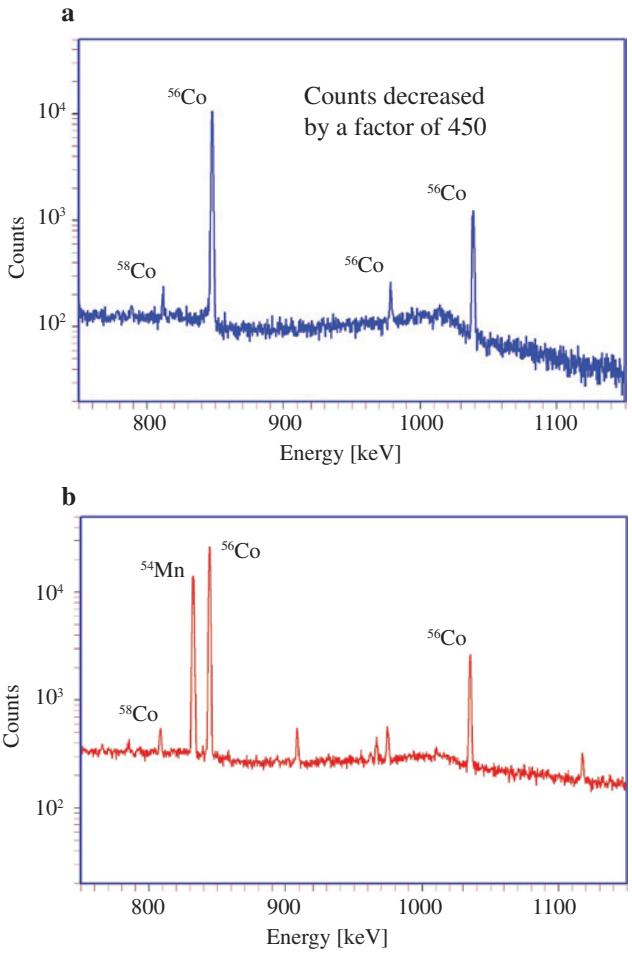

Figure 1: Part of the γ-ray spectrum, (a) of natural iron target irradiated with protons, (b) of radiochemically separated radiomanganese fraction.

For each separated sample, the ^{54}Mn count rate obtained had to be corrected for two experimental parameters:

(a) Extended source effect. Two relatively strong samples were counted directly on the surface of the detector and at a distance of 10 cm. By a comparison of the count rates and considering the efficiencies at the two positions, a correction factor for the extended nature of the source was determined.

(b) Yield of chemical separation. While chemically processing two irradiated Fe foils, a very small quantity of the radionuclide ^{52}Mn ($T_{1/2}$ = 5.6 d; E_γ = 1434 keV; I_γ = 100 %) was mixed as a radioactive tracer. This radionuclide was produced in no-carrier- added form separately at the cyclotron BC 1710 via the ^{52}Cr(p,n)^{52}Mn reaction as described earlier [25, 32]. By a comparison of the ^{52}Mn activity before and after the chemical separation, the yield of separation was determined. On average it amounted to 75 ± 3 %.

After the above mentioned two corrections, the count rate of ^{54}Mn was treated the same way as for other reaction products obtained non-destructively.

2.4 Proton flux measurement

The proton beam flux was measured by charge integration before reaching the target. The beam flux effective in the target was determined exactly via the monitor reactions ^{nat}Cu(p,x)^{62}Zn and ^{nat}Cu(p,x)^{65}Zn induced in the Cu-foil mounted in front of each stack. The standard cross section values for the above monitor reactions were taken from the IAEA recommended excitation functions [27]. The flux values from the above two monitor reactions agreed within 6 %. The average of the two values was used to calculate the reaction cross section. This value was treated as constant over the stack.

2.5 Calculation of cross section and estimation of uncertainty

The count rate of each product radionuclide was converted to decay rate by applying the usual corrections, like the intensity of the γ-ray used, the efficiency of the detector, pile-up and coincidence loss, etc. and thereafter extrapolated to the end of bombardment (EOB). From the decay rate at EOB and the proton flux determined via the monitor reaction, the radionuclide production cross section was calculated using the well-known activation equation. The overall uncertainty in the cross section was obtained by a quadratic summing of the individual uncertainties, namely counting statistics (0.1–7 %), spectrum analysis (0.5–5 %), efficiency of the detector (4 %), half-life of the product (0.1–1.6 %), γ-ray intensity (0.2–6 %), coincidence loss (<0.5 %) and monitor reaction cross section (6 %). The uncertainty in the number of target nuclei of <1 % was also included. For chemically separated samples a further uncertainty of 5 % in the separation yield was added. In general, the overall uncertainties associated with the measured cross sections were between 7 and 14 %.

Table 2: Cross sections for the formation of the radionuclides $^{56,57,58m+g}$Co and ^{54}Mn in interactions of protons with ^{nat}Fe, measured non-destructively via γ-ray spectrometry.

Proton energy (MeV)[a]	Cross section (mb)			
	^{56}Co	^{57}Co	$^{58m+g}$Co	^{54}Mn
15.7 ± 0.2	184 ± 13	4.8 ± 0.3	0.54 ± 0.05	1.11 ± 0.10
15.4 ± 0.2	200 ± 14	4.8 ± 0.3	0.56 ± 0.05	1.25 ± 0.12
15.0 ± 0.2	225 ± 16	5.4 ± 0.4	0.66 ± 0.06	1.11 ± 0.10
14.3 ± 0.2	288 ± 18	5.2 ± 0.4	1.06 ± 0.09	
13.8 ± 0.2	283 ± 20	5.7 ± 0.4	1.14 ± 0.08	1.13 ± 0.10
13.7 ± 0.2	312 ± 22	6.1 ± 0.4	1.23 ± 0.11	1.15 ± 0.11
12.9 ± 0.2	333 ± 23	7.6 ± 0.5	1.45 ± 0.13	0.90 ± 0.09
12.9 ± 0.2	334 ± 16	6.8 ± 0.5	1.25 ± 0.08	
12.0 ± 0.3	326 ± 23	8.5 ± 0.6	1.78 ± 0.13	0.86 ± 0.08
11.4 ± 0.3	343 ± 24	11.0 ± 0.8	2.04 ± 0.18	0.79 ± 0.07
11.2 ± 0.3	350 ± 22	9.7 ± 0.8	2.16 ± 0.16	
10.4 ± 0.3	331 ± 23	11.6 ± 0.8	1.99 ± 0.17	0.53 ± 0.05
10.0 ± 0.3	306 ± 21	11.6 ± 0.8	1.83 ± 0.14	0.61 ± 0.06
9.9 ± 0.3	318 ± 20	11.5 ± 0.8	2.02 ± 0.14	
8.7 ± 0.3	284 ± 20	11.4 ± 0.8	1.90 ± 0.18	0.49 ± 0.05
8.3 ± 0.3	269 ± 17	10.3 ± 0.8	1.80 ± 0.14	
7.9 ± 0.3	237 ± 17	10.8 ± 0.8	1.72 ± 0.13	
7.8 ± 0.3	236 ± 15	9.4 ± 0.7	1.45 ± 0.10	
7.7 ± 0.4	232 ± 16	10.7 ± 0.8	1.71 ± 0.16	
6.8 ± 0.4	175 ± 12	8.5 ± 0.6	1.45 ± 0.10	
6.4 ± 0.4	129 ± 9	8.2 ± 0.6	1.24 ± 0.10	
6.1 ± 0.4	117 ± 8	8.0 ± 0.6	1.28 ± 0.10	
5.8 ± 0.2	85 ± 6	7.5 ± 0.5	1.00 ± 0.10	
5.7 ± 0.2	57 ± 11	7.1 ± 0.5	0.78 ± 0.05	
5.1 ± 0.2	8.7 ± 0.6	6.6 ± 0.5	0.43 ± 0.03	
4.8 ± 0.2		6.0 ± 0.4	0.34 ± 0.03	
4.7 ± 0.2		5.9 ± 0.4	0.32 ± 0.03	
4.5 ± 0.2		5.0 ± 0.3	0.26 ± 0.02	
4.4 ± 0.2		4.8 ± 0.3	0.24 ± 0.02	
4.1 ± 0.3		4.0 ± 0.3	0.19 ± 0.02	
4.0 ± 0.3		3.8 ± 0.3	0.18 ± 0.02	
3.7 ± 0.3		3.0 ± 0.2	0.14 ± 0.01	
3.6 ± 0.3		2.7 ± 0.2	0.11 ± 0.01	
3.5 ± 0.3		2.2 ± 0.2	0.08 ± 0.01	
3.4 ± 0.3		1.7 ± 0.1	0.08 ± 0.01	
3.3 ± 0.3		1.4 ± 0.1	0.04 ± 0.004	
3.0 ± 0.3		1.0 ± 0.1	0.02 ± 0.003	
2.9 ± 0.3		1.0 ± 0.1	0.03 ± 0.004	
2.4 ± 0.3		0.5 ± 0.04	0.01 ± 0.002	

[a]The deviation given here describes the energy spread within each foil.

3 Results and discussion

The cross sections for the formation of the radionuclides $^{56,57,58m+g}$Co and ^{54}Mn via proton induced nuclear reactions on ^{nat}Fe, measured non-destructively in this work from the respective threshold to 16 MeV, are summarized in Table 2. The estimated uncertainties in the measured cross sections and the energy spread in each foil are also presented. The data on the formation of ^{54}Mn obtained radiochemically are given separately in Table 3. The excitation functions of the investigated nuclear reactions are shown in Figures 2–5. Curve fitting to all the experimental data sets available in literature, including this work, was performed with high order polynomials. The present data were also fitted individually. The best fitting was

Table 3: Radiochemically measured cross sections of the $^{nat}Fe(p,x)^{54}Mn$ process.

Proton energy (MeV)[a]	Cross section (mb)
14.3±0.2	1.08±0.12
12.9±0.2	0.80±0.10
11.2±0.3	0.62±0.08
9.9±0.3	0.42±0.06
8.3±0.3	0.41±0.06
7.8±0.3	0.24±0.03
6.4±0.40	0.16±0.02
5.8±0.40	0.07±0.01

[a]The deviation given here describes the energy spread within each foil.

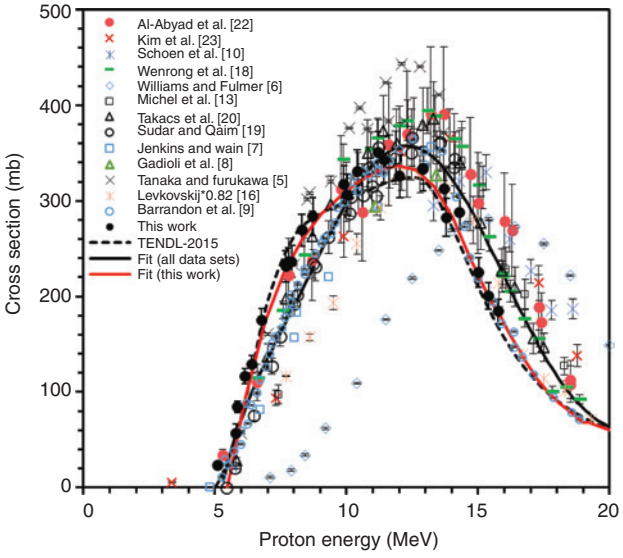

Figure 2: Excitation function of the $^{nat}Fe(p,xn)^{56}Co$ reaction.

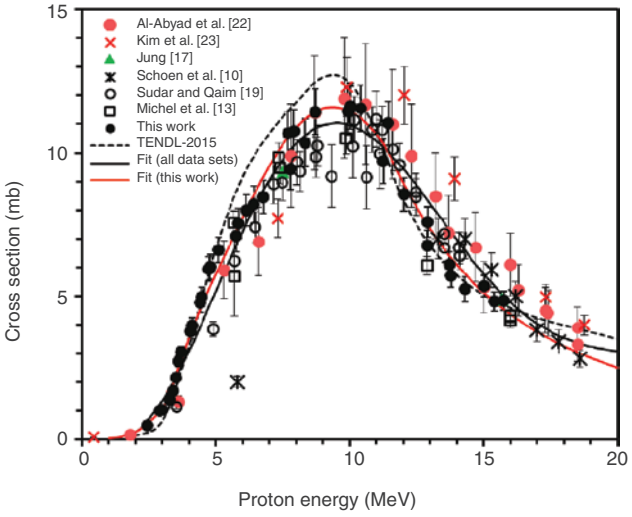

Figure 3: Excitation function of the $^{nat}Fe(p,x)^{57}Co$ reaction.

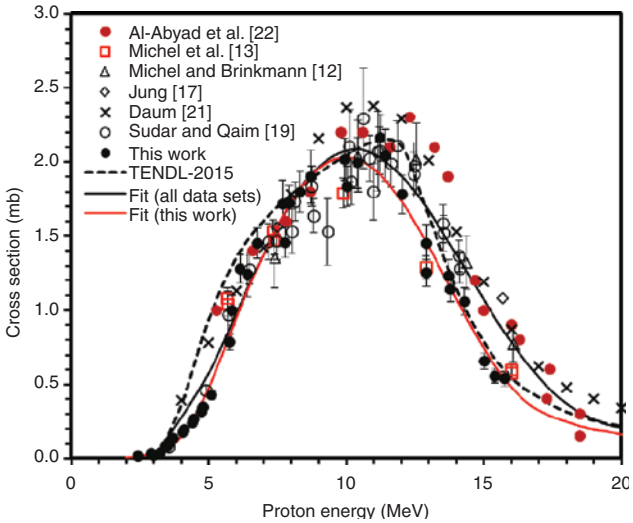

Figure 4: Excitation function of the $^{nat}Fe(p,x)^{58m+g}Co$ reaction.

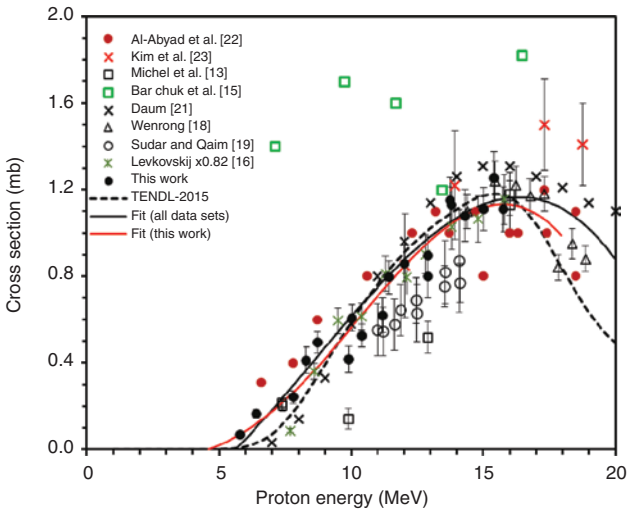

Figure 5: Excitation function of the $^{nat}Fe(p,x)^{54}Mn$ reaction.

obtained with the polynomials from 3rd to 5th order. Both fitted curves are also shown in the figures. The theoretically calculated values were taken from the TENDL-2015 library [33]. Those values are based on the TALYS code which takes into account the contributions of both compound and precompound processes, besides considering the nuclear structure of the produced radionuclides.

3.1 $^{nat}Fe(p,xn)^{56}Co$

Our measured cross sections for the formation of ^{56}Co in the interaction of protons with iron of natural isotopic

composition are shown in Figure 2. The available experimental data and theoretical values from the TENDL-2015 library are also given. The contribution of the ^{57}Fe(p,2n)^{56}Co process (E_{thr}=13.23 MeV) should be negligible in our investigated energy range because of low abundance of ^{57}Fe in ^{nat}Fe. Sudár and Qaim [19] reported the contribution of the above process as about 2 % up to 18 MeV proton energy. The major contribution to the formation of ^{56}Co thus comes from the ^{56}Fe(p,n)^{56}Co reaction. The data sets for the ^{56}Fe(p,n)^{56}Co process, based on measurement on the enriched ^{56}Fe target, could thus be converted to natural target over our investigated energy range. On this basis the data by Jenkins and Wain [7], Tanaka and Furukawa [5], Gadioli et al. [8] and Levkovskij [16] were normalized to natural target. In the latter case a reduction factor of 0.82 was also applied as suggested by Qaim et al. [34]. Our values are in agreement with many of the data sets within the experimental errors. A significant deviation was found only from the data of Tanaka and Furukawa [5], their values being 12–22 % higher around the peak of the excitation function than our values. The data by Kim et al. [23] and Schoen et al. [10] appear to be high in the higher energy range and those by Jenkins and Wain [7] and Levkovskij [16] are low in the low energy region. In contrast, the data by Williams and Fulmer [6] are not comparable to this work because they show a large energy shift of 3–4 MeV. In more detail, our data in the energy range of 7–9 MeV are slightly higher than the other values and beyond the peak, i. e. between 13 and 15 MeV, somewhat lower than most of the literature values. Nonetheless, our data are in much better agreement with the theoretically calculated TENDL-2015 curve than the fitted curve to all the available data. The database near the reaction threshold is strengthened, but a critical evaluation of all data appears necessary.

3.2 ^{nat}Fe(p,x)^{57}Co

The measured cross sections for the formation of ^{57}Co are shown in Figure 3. The decay of ^{57}Co is followed by the emission of 122 keV and 136 keV gamma rays. Both gamma rays lie in the energy range over which the efficiency curve of the HPGe detector is very sensitive; therefore, a reliable calibration of the detector was essential. A few groups [10, 13, 18, 19, 22, 23] reported data on the ^{57}Co production. Those data sets and the data compiled in the library TENDL-2015 are also shown in Figure 3. Our data are generally in good agreement with the other experimental data, except for a few data points which show deviation; for example, in the peak energy region the data by Sudár and Qaim [19] are slightly lower than the others, and just beyond the peak energy the data by Al-Abyad et al. [22] and Kim et al. [23] are somewhat higher.

Three competing channels contribute to the production of ^{57}Co in our investigated energy range. From the report in TENDL-2015 library the (p,γ) process contributes to ^{57}Co production up to about 80 % below 3 MeV. Thereafter the contribution of the competing (p,n) channel rises sharply with the increasing energy and reaches a maximum value at around 9 MeV. At this energy the contribution of the (p,γ) process is only 3 %. A visible contribution of the (p,2n) process appears at about 13 MeV and at this energy the individual contributions of the (p,γ), (p,n) and (p,2n) processes to the production of ^{57}Co from ^{nat}Fe are about 11 %, 82 % and 7 %, respectively. The low contribution of the (p,2n) process is due to its high threshold as well as due to the low isotopic abundance (0.282 %) of the target isotope ^{58}Fe in natural target.

Our results considerably strengthen the database up to 5 MeV and show good agreement with the theoretical calculations, except for the energy range between 5 and 8 MeV where the theory predicts somewhat higher values, possibly due to an overestimation of the ^{56}Fe(p,n)^{57}Co reaction cross section near its threshold.

3.3 ^{nat}Fe(p,x)$^{58m+g}$Co

The radionuclide ^{58}Co has two isomeric states, a long-lived ground state ^{58g}Co ($T_{1/2}$=70.86 d) and a metastable state ^{58m}Co ($T_{1/2}$=9.15 h). The metastable state decays by 100 % isomeric transition to the ground state. The 810.8 keV γ-ray emitted in the decay of ^{58g}Co was measured after complete decay of ^{58m}Co to the ground state. Thus the measured cross section describes the cumulative formation of ^{58g}Co. The measured excitation function is shown in Figure 4 together with the available literature values and model calculation reported in the TENDL-2015 library. Two competing channels, namely (p,γ) and (p,n), contribute to the production of ^{58}Co. The TENDL-2015 library shows the contribution of the former process to be low in comparison to the latter one. Sudár and Qaim [19] reported cross sections of the ^{58}Fe(p,n)^{58m,g}Co reaction based on measurements using ^{nat}Fe but normalized to the isotopic abundance of ^{58}Fe. Those values were now renormalized to the natural target and the results are shown in Figure 4. Our data are in good agreement with most of the literature values within uncertainty limits, except for the data by Daum [21] which are consistently higher, presumably due to preliminary nature of those data. The agreement between the fitted curves obtained from all experimental

data (including this work) and that from only this work is excellent up to 12 MeV, although the TENDL-2015 values are rather high between 4 and 7 MeV. Thereafter, the fitted curve to present data becomes lower than the fit to all data. However, our data agree both in magnitude and shape with the TENDL-2015 curve in the upper energy region.

An important aspect of our measurements is the significant strengthening of the database in the low energy region below 5 MeV.

3.4 $^{nat}Fe(p,x)^{54}Mn$

The measured cross sections for the formation of the radionuclide ^{54}Mn ($T_{1/2}$ = 312.3 d) in the interaction of protons with ^{nat}Fe target, obtained by both non-destructive γ-ray spectrometry and radiochemical analysis, are shown in Figure 5. The radionuclide ^{54}Mn is possibly produced to a major extent via the $^{57}Fe(p,\alpha)^{54}Mn$ channel on iron of natural isotopic composition, the contribution of the $^{58}Fe(p,\alpha n)^{54}Mn$ process being negligibly small due to low % of ^{58}Fe and high threshold of the reaction. Due to low isotopic abundance of ^{57}Fe (2.119 %) and long half-life of ^{54}Mn, the activity produced was very low and only a weak peak appeared in the γ-ray spectrum of samples irradiated with >8.5 MeV protons. Therefore, more uncertainties due to poor counting statistics and peak area analysis were added to the measured cross section values. In the lower energy range investigated by the radiochemical technique, however, even very low cross sections could be measured with reasonable accuracy. Al-Abyad et al. [22] determined the ^{54}Mn formation cross sections from enriched ^{57}Fe and also extrapolated the values from ^{nat}Fe taking into account the isotopic abundance of ^{57}Fe in natural iron. Their values are shown in Figure 5 after normalization to natural target. Our values measured above 8.5 MeV are consistent with those values, except for some scatter in their data. Our data in the lower energy range are somewhat lower than those values but higher than the data by Daum [21] and Levkovskij [16]. Comparing our results with other data we find that the values by Sudár and Qaim [19] are systematically lower by about 20 % and the data by Michel et al. [13] show large deviations. The data by Barchuk et al. [15] are so high that they are not comparable to our values as well as to other literature values. Daum [21] data in the energy region beyond 15 MeV are also rather high. As regards TENDL-2015 library, the present data show good agreement with the theoretical curve over the investigated proton energy range.

Our radiochemical results, especially those below 8.3 MeV, considerably strengthen the database and establish the reaction threshold at about 5.6 MeV.

4 Conclusion

Excitation functions of the proton induced nuclear reactions on iron leading to the formation of the radionuclides ^{56}Co, ^{57}Co, $^{58m+g}Co$ and ^{54}Mn were measured from threshold to 16 MeV. New detailed results near threshold energy have been obtained for all the four radionuclides. They allowed to deduce exact reaction thresholds of those long-lived activation products. The other data are of confirmatory nature and strengthen the database. The fitted curves to our data generally agree well with the theoretically calculated results given in TENDL-2015. The major contribution to each investigated reaction thus appears to be furnished by a combination of statistical and precompound processes.

Acknowledgements: This joint project was partly funded by the Alexander von Humboldt Foundation of Germany (grant recipient Md. Shuza Uddin in Bangladesh) for which we are grateful. We thank Prof. B. Neumaier, the Director of Nuclear Chemistry at FZ Jülich, Germany for his support of the long-term cooperation. We are grateful to the operational crew of the BC 1710 for performing the irradiations as well as to A. Thesing, K. Giesen and U. Königs, all at FZ Jülich, for assistance in radiochemical studies.

References

1. Qaim, S. M.: Nuclear data relevant to the production and application of diagnostic radionuclides. Radiochim. Acta **89**, 223 (2001).
2. Qaim, S. M.: Nuclear data for production and medical application of radionuclides: present status and future needs. Nucl. Med. Biol. **44**, 31 (2017).
3. Uddin, M. S., Sudár, S., Spahn, I., Shariff, M. A., Qaim, S. M.: Excitation function of the $^{60}Ni(p,\gamma)^{61}Cu$ reaction from threshold to 16 MeV. Phys. Rev. C **93**, 044606 (2016).
4. Qaim, S. M., Sphan, I., Scholten, B., Neumaier, B.: Uses of alpha particles, especially in nuclear reaction studies and medical radionuclide production. Radiochim. Acta **104**, 601 (2016).
5. Tanaka, S., Furukawa M.: Excitation functions for (p,n) reactions with titanium, vanadium, chromium, iron and nickel up to 14 MeV. J. Phys. Soc. Japan **14**, 1269 (1959).
6. Williams, I. R., Fulmer, C. B.: Excitation functions for radioactive isotopes produced by protons below 60 MeV on Al, Fe, and Cu. Phys. Rev. **162**, 1055 (1967).
7. Jenkins, I. L., Wain, A. G.: Excitation functions for the bombardment of Fe-56 with protons. J. Inorg. Nucl. Chem. **32**, 1419 (1970).
8. Gadioli, E., Grassistrini, A. M., Lobianco, G., Strini, G., Tagliaferri, G.: Excitation functions of V-51, Fe-56, Cu-65(p,n) reactions between 10 and 45 MeV. Nuovo Cimento A **22**, 547 (1974).
9. Barrandon, J. N., Debrun, J. L., Kohn, A., Spear, R. H.: A study of the main radioisotopes obtained by irradiation of Ti, V, Cr, Fe, Ni, Cu and Zn with protons from 0 to 20 MeV. Nucl. Instrum. Methods Phys. Res. **127**, 269 (1975).

10. Schoen, N. C., Oriov, G., Mcdonald, R. J.: Excitation functions for radioactive isotopes produced by proton bombardment of Fe, Co and W in the energy range from 10 to 60 MeV. Phys. Rev. C **20**, 88 (1979).
11. Boukharouba, N., Brient, C. E., Grimes, S. M., Mishra, V., Pedroni, R. S.: Low energy optical model studies of proton scattering on ^{54}Fe and ^{56}Fe. Phys. Rev. C **46**, 2375 (1992).
12. Michel, R., Brinkmann, G.: On the depth-dependent production of radionuclides ('A' between 44 and 59) by solar protons in extraterrestrial matter. J. Radioanal. Chem. **59**, 467 (1980).
13. Michel, R., Bodemann, R., Busemann, H., Daunke, R., Gloris, M., Lange, H.-J., Klug, B., Krins, A., Leya, I., Luepke, M., Neumann, S., Reinhardt, H., Schnatz-Buettgen, M., Herpers, U., Schiekel, Th., Sudbrock, F., Holmqvist, B., Conde, H., Malmborg, P., Suter, M., Dittrich-Hannen, B., Kubik, P. W., Synal, H. A., Filges, D.: Cross sections for the production of residual nuclides by low- and medium-energy protons from the target elements C, N, O, Mg, Al, Si, Ca, Ti, V, Mn, Fe, Co, Ni, Cu, Sr, Y, Zr, Nb, Ba and Au. Nucl. Instrum. Meth. Phys. Res. B **129**, 153 (1997).
14. Kennett, S. R., Mitchell, L. W., Anderson, M. R., Sargood, D. G.: Cross-section measurements and thermonuclear reaction rates for ^{52}Cr(p,γ)^{53}Mn and ^{54}Fe(p,γ)^{55}Co. Nucl. Phys. A **363**, 233 (1981).
15. Barchuk, I. F., Bulkin, V. S., Kuzmenkova, V. A., Kurilo, P. M., Lobach, Y. N. Ogorodnik, A. F., Procopenko, V. S., Sklyarenko, V. D., Tokarevsky, V. V.: Excitation functions of the reactions induced by interactions of protons over an energy range up to 67 MeV with silicon and iron nuclei. Atomnaya Energiya **63**, 30 (1987).
16. Levkovskij, V. N.: Activation cross sections of nuclides of average masses (A = 40–100) by protons and alpha-particles with average energies (E = 10–50 MeV), Inter-Vesi, Moscow (1991).
17. Jung, P.: Cross sections for the production of helium and long- living radioactive isotopes by protons and deuterons. Proc. Int. Conf. on Nucl. Data for Sci. and Technol., Jülich, Germany (Edited by S. M. Qaim, F. Z. Jülich), Springer Verlag, Heidelberg, p. 352 (1992).
18. Wenrong, Z., Hanlin, L., Weixiang, Y.: Measurement of cross sections by bombarding Fe with protons up to 19 MeV. Chinese J. Nucl. Phys. (Beijing) **15**, 337 (1993).
19. Sudár, S., Qaim, S. M.: Excitation functions of proton and deuteron induced reactions on iron and alpha-particle induced reactions on manganese in the energy region up to 25 MeV. Phys. Rev. C **50**, 2408 (1994).
20. Takács, S., Vasvary, L., Tárkányi, F.: Remeasurement and compilation of excitation function of proton induced reactions on iron for activation techniques. Nucl. Instrum. Methods Phys. Res. B **89**, 88 (1994).
21. Daum, E.: Investigation of light ion induced activation cross sections in iron. Proton induced activation cross sections. Fed. Rep. Germany, Progress Report (Edited by S. M. Qaim, FZ Jülich), Jül-Report-3410; INDC (Germany), No.043, p. 4–5 (1997).
22. Al-Abyad, M., Comsan, M. N. H., Qaim, S. M.: Excitation functions of proton-induced reactions on ^{nat}Fe and enriched ^{57}Fe with particular reference to the production of ^{57}Co. Appl. Radiat. Isot. **67**, 122 (2009).
23. Kim, K. S., Khandaker, M. U., Naik, H., Kim G. N.: Excitation functions of proton induced reactions on ^{nat}Fe in the energy region up to 45 MeV. Nucl. Instrum. Methods Phys. Res. B **322**, 63 (2014).
24. Uddin, M. S., Chakraborty, A. K., Spellerberg, S., Shariff, M. A., Das, S., Rashid, M. A., Spahn, I., Qaim, S. M.: Experimental determination of proton induced reaction cross sections on ^{nat}Ni near threshold energy. Radiochim. Acta **104**, 305 (2016).
25. Spellerberg, S., Scholten, B., Spahn, I., Bolten, W., Holzgreve, M., Coenen, H. H., Qaim, S. M.: Target development for diversified irradiations at a medical cyclotron. Appl. Radiat. Isot. **104**, 106 (2015).
26. Piel, H., Qaim, S. M., Stöcklin, G.: Excitation functions of (p,xn) reactions on ^{nat}Ni and highly enriched ^{62}Ni: possibility of production of medically important radioisotope ^{62}Cu at a small cyclotron. Radiochim. Acta **57**, 1 (1992).
27. Tárkányi, F., Takács, S., Gul, K., Hermanne, A., Mustafa, M. G., Nortier, M., Obložinský, Qaim, S. M., Scholten, B., Shubin, Yu. N., Youiang, Z.: Beam monitor reactions: in charged particle cross section database for medical radioisotope production. IAEA-TECDOC-1211, p. 49 (2001).
28. Williamson, C. F., Boujot, J. P., Picard, J.: Tables of range and stopping power of chemical elements for charged particles of energies from 0.5 to 500 MeV. Report CEA-R 3042 (1966).
29. Chu, S. Y. F., Ekström, L. F., Firestone, R. B.: Lund/LBNL Nuclear Data Service, Version 2.0. (1999) http://nucleardata.nuclear.lu.se/nucleardata/toi/.
30. Zaman, M. R., Spellerberg, S., Qaim, S. M.: Production of ^{55}Co via the ^{54}Fe(d,n)-process and excitation functions of ^{54}Fe(d,t)^{53}Fe and ^{54}Fe(d,α)^{52m}Mn reactions from threshold up to 13.8 MeV. Radiochim. Acta **91**, 105 (2003).
31. Qaim, S. M., Wölfle, R., Stöcklin, G.: Radiochemical methods in the determination of nuclear data for fusion reactor technology. J. Radioanalyt. Chem. **30**, 35 (1976).
32. Buchholz, M., Spahn, I., Scholten, B., Coenen, H. H.: Cross section measurements for the formation of manganese-52 and its isolation with a non-hazardaus eluent. Radiochim. Acta **101**, 491 (2013).
33. Koning, A. J., Rochman, D., van der Marck, S. C., Kopecky, J., Sublet, J. Ch., Pomp, S., Sjostrand, H., Forrest, R., Bauge, E., Henriksson, H., Cabellos, O., Goriely, S., Leppanen, I., Leeb, H., Plompen, A., Mills, R.: TENDL-2015: TALYS-based evaluated nuclear data library (release date: 18 January 2016, last update: 5 October 2016). https://tendl.web.psi.ch/tendl_2015/tendl2015.html.
34. Qaim, S. M., Sudár, S., Scholten, B., Koning, A. J., Coenen, H. H.: Evaluation of excitation functions of ^{100}Mo(p, d + pn)^{99}Mo and ^{100}Mo(p, 2n)^{99m}Tc reactions: estimation of long-lived Tc-impurity and its implication on the specific activity of cyclotron-produced ^{99m}Tc. Appl. Radiat. Isot. **85**, 101 (2014).